Paleoceanography and Paleoclimatology

Supporting Information for

Magnetic fingerprints for the paleoenvironmental evolutions since the last deglaciation: evidence from the northwestern South China Sea sediment

Qishun Sun[1], Zhaoxia Jiang[1,2*], Chunfeng Xiao[1], Long Chen[1], Wanxin Liu[1], Kuang He[1,2], Yulong Guan[1], Yuzhen Zhang[1], Haosen Wang[3], Liang Chen[4], Zhengxin Yin[4], Sanzhong Li[1,2]

[1]Frontiers Science Center for Deep Ocean Multispheres and Earth System, Key Laboratory of Submarine Geosciences and Prospecting Techniques, Ministry of Education, Chongben Honors College, College of Marine Geosciences, Ocean University of China, Qingdao 266100, P.R. China

[2]Laboratory for Marine Geology, and Laboratory for Marine Mineral Resources, Laoshan National Laboratory, Qingdao 266237, P.R. China

[3]Center for Marine Magnetism (CM^2), Department of Ocean Science and Engineering, Southern University of Science and Technology, Shenzhen 518055, PR China

[4]South China Sea Marine Survey and Technology Center, State Oceanic Administration, Guangzhou 510300, China

[*]Corresponding author:

Z. Jiang,

jiangzhaoxia@ouc.edu.cn

Contents of this file

Introduction

The supporting information contains the Figures S1 to S8, and Tables S1 to S2. Table S1 reports the age-depth tie points for the age model. Table S2 records the results of principal component analysis (PCA) of major elements.

Supplementary Figures

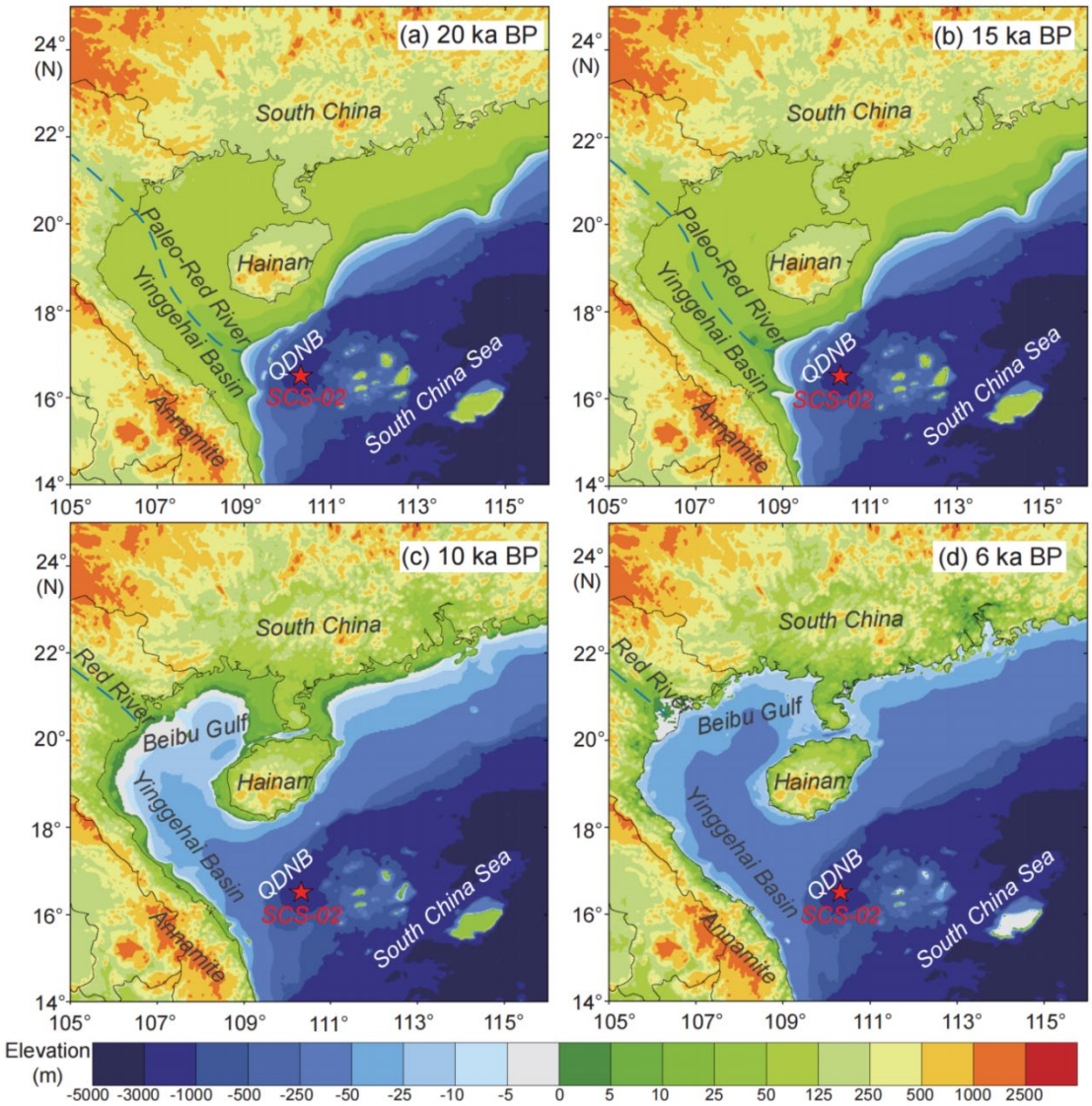

Figure S1. The shoreline changes of northwestern SCS since 20 ka BP (modified from Yao et al., 2009). The QDNB represents Qiongdongnan basin.

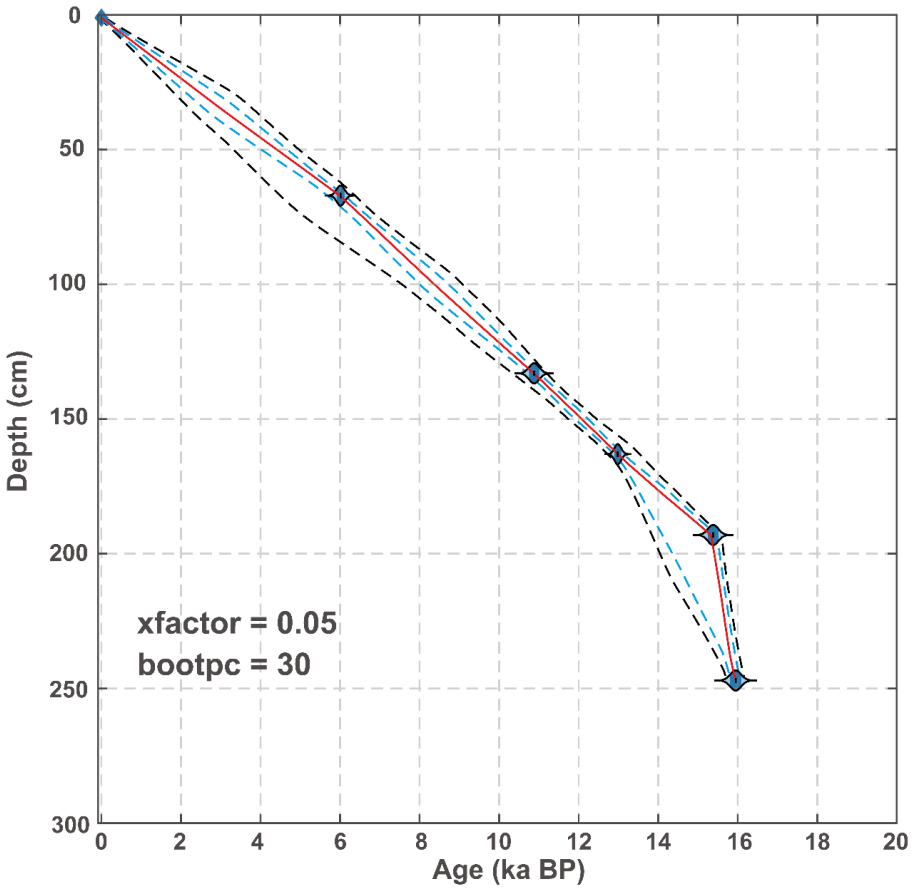

Figure S2. Age model in core SCS-02. The red line represents the linear interpolation age. The age of core SCS-02 is constrained by five AMS ^{14}C dates, which were measured at Beta Analytic Laboratory (USA). The AMS ^{14}C dates were converted to calendar years using the Marine20 (Heaton et al., 2020) in *Calib 8.20* program with additional regional reservoir age of -135 ± 47 yr acquired from Xisha islands. Uncertainties in the age model of core SCS-02 were estimated using the software *Undatable* (Lougheed & Obrochta, 2019), with parameters of xfactor = 0.05 and bootpc = 30. The blue and black dashed line represent 1σ and 2σ age uncertainties calculated by sofware *Undatable* (Lougheed & Obrochta, 2019).

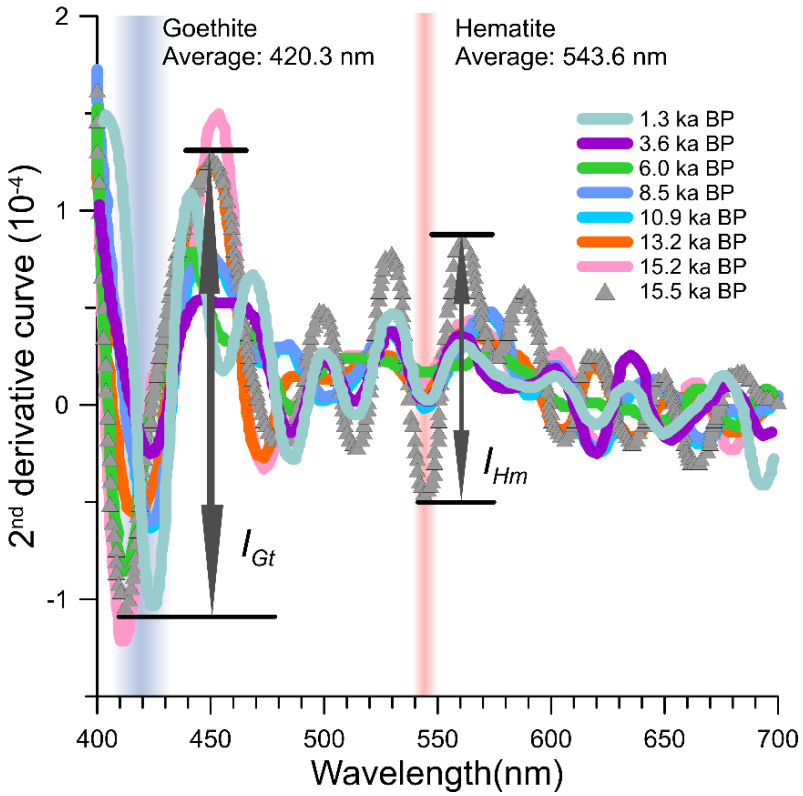

Figure S3. The second derivative of diffuse reflectance spectroscopy (DRS) of typical samples in core SCS-02. The blue bar and red bar indicate the characteristic peak positions for goethite (P_{Gt}) and hematite (P_{Hm}), respectively. The hematite (I_{Hm}) and goethite (I_{Gt}) band intensities that are the ordinate differences between the minimum and the next longer wavelength maximum are showed with bidirectional arrows using the sample of 15.5 ka BP as example. The I_{Gt} and I_{Hm} are proportional to the goethite and hematite concentration, respectively.

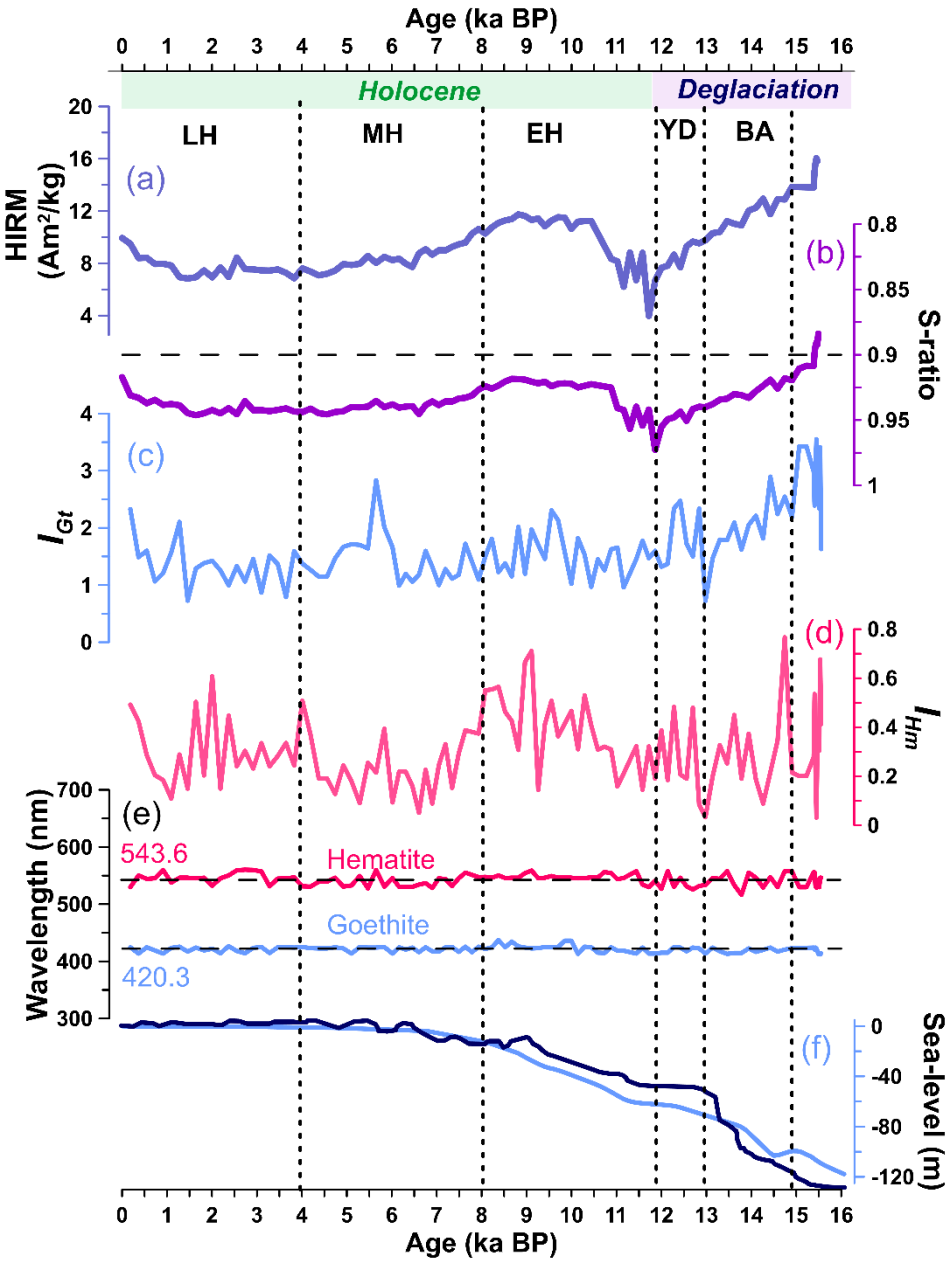

Figure S4. Related parameters of hematite and goethite. (a) HIRM, the "hard" isothermal remanent magnetization; (b) S-ratio; (c-d) I_{Gt} and I_{Hm}, intensity of goethite and hematite acquired from the second derivative of K-M remission function from DRS; (e) Wavelength band of hematite and goethite obtained from DRS results, and the average bands are 543.6 nm (hematite) and 420.3 nm (goethite), respectively; (f) global (blue line) and northwestern South China Sea (black line) sea-level curves (Lambeck et al., 2014; Yao et al., 2009).

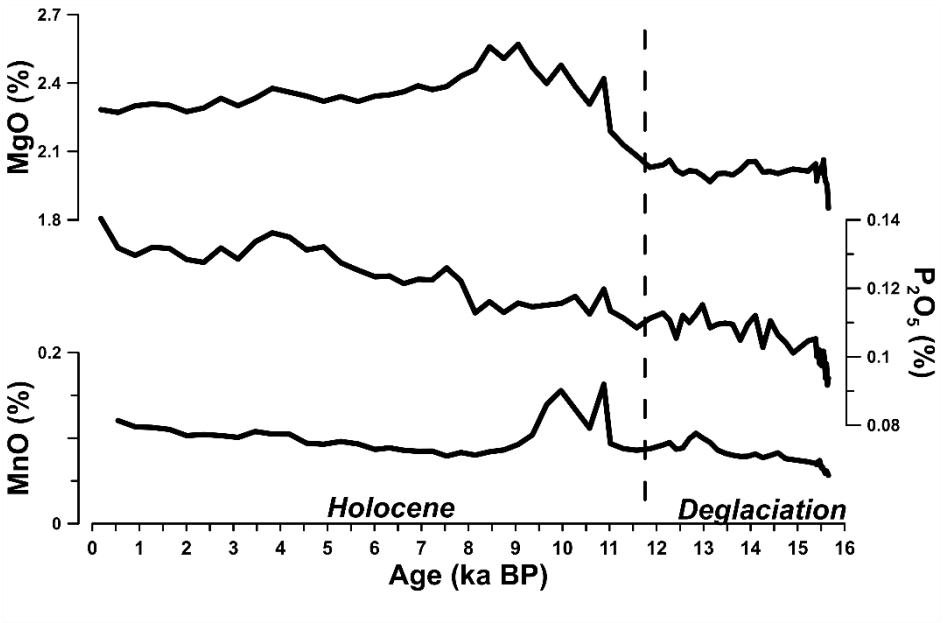

Figure S5. The other major elements not mentioned in the manuscript.

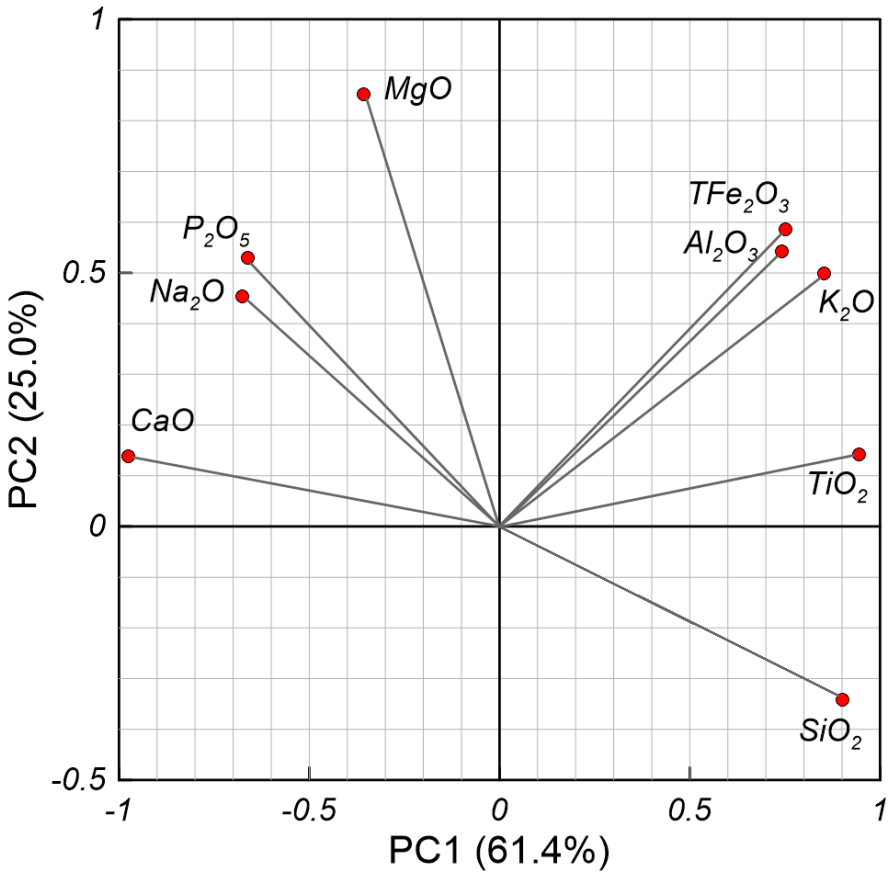

Figure S6. Biplot of the first two principal components (PC1 and PC2) with loadings of the anayzed major elements.

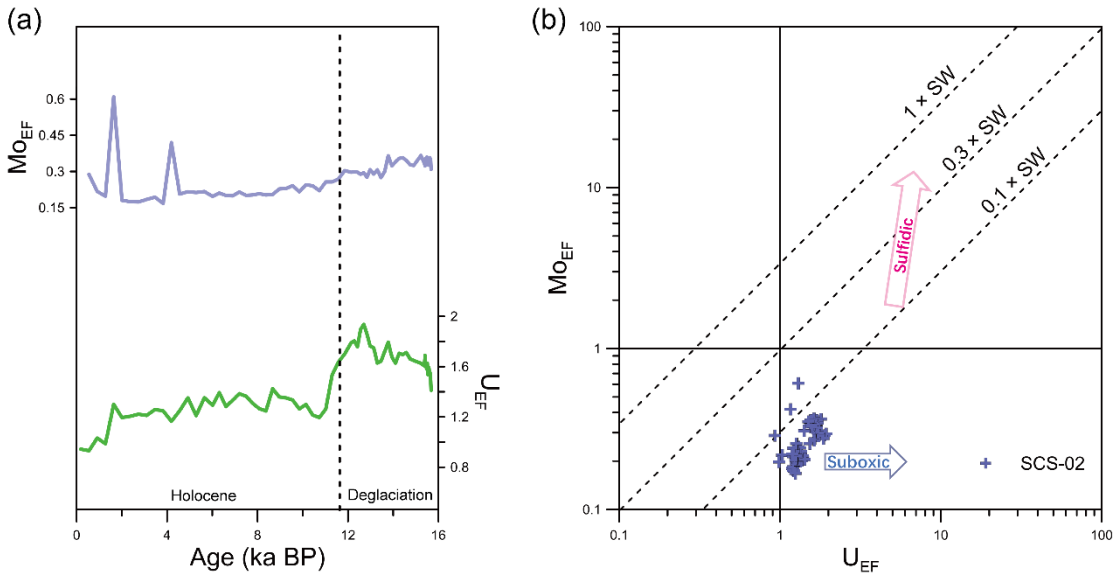

Figure S7. Redox proxies of core SCS-02. (a) the temporal variations of redox proxies including Mo and U enrichment factors (higher values correspond to more reduction); (b) The scatter of Mo and U enrichment factors of SCS-02.

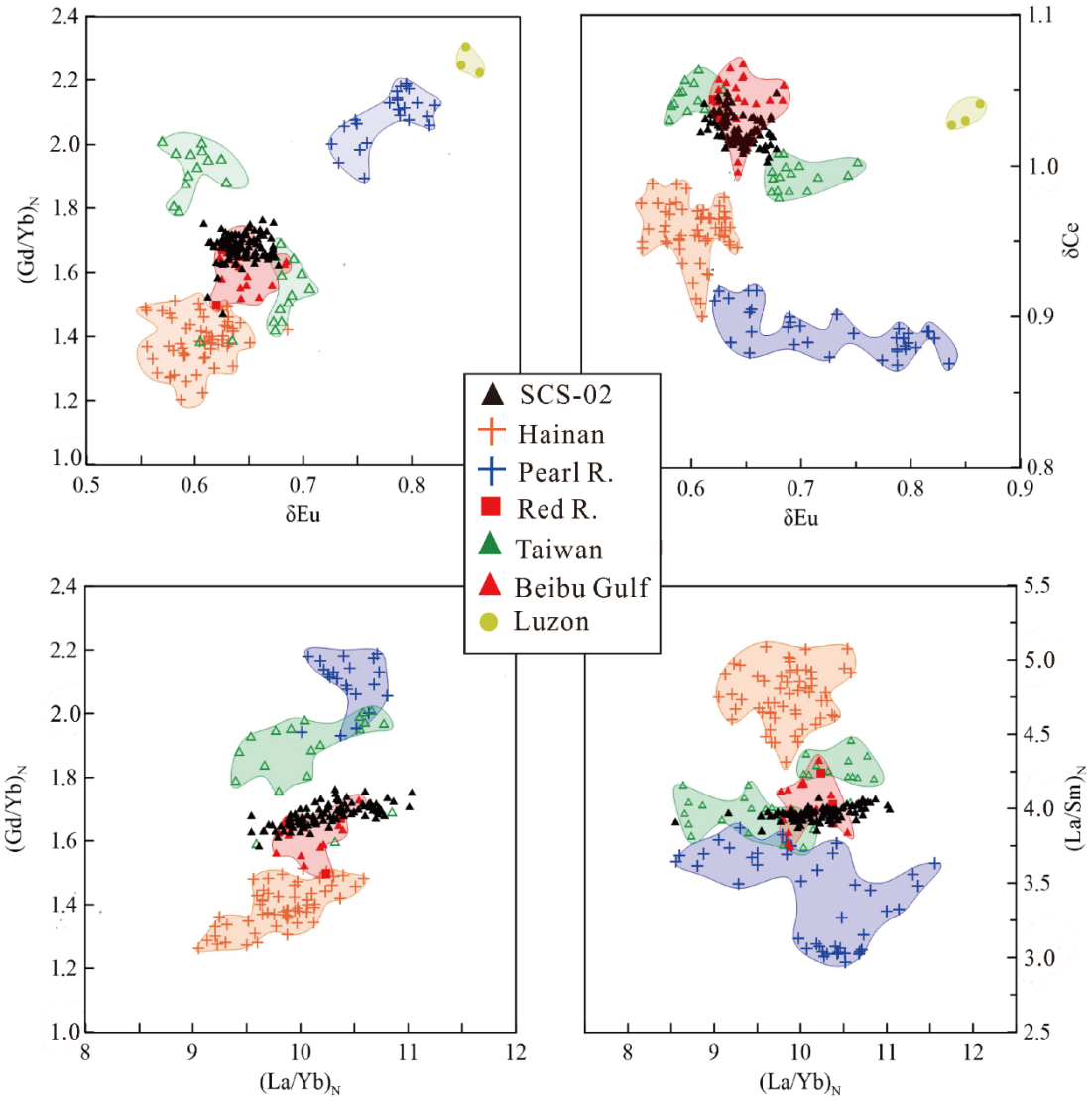

Figure S8. Provenance indication of rare earth elements for core SCS-02 in our previous study (Xiao et al., 2023). Rare earth signatures, including Eu anomaly (δEu), Ce anomaly (δCe), and the chondrite normalized $(Gd/Yb)_N$, $(La/Yb)_N$, and $(La/Sm)_N$ were applied. The SCS-02 samples (black triangle) were more similar to those of the Red River and Beibu Gulf samples.

Table S1.

Radiocarbon ages from core SCS-02

Sample ID	Depth (cm)	Materials	AMS ^{14}C Ages (ka BP)	2σ
SCS02-12	66-68	*G. sacculifer* & *G. ruber*	6.015	5.823-6.206
SCS02-23	132-134	*G. sacculifer* & *G. ruber*	10.879	10.646-11.112
SCS02-28	162-164	*G. sacculifer* & *G. ruber*	12.977	12.800-13.153
SCS02-33	192-194	*G. sacculifer* & *G. ruber*	15.385	15.128-15.641
SCS02-42	246-248	*G. sacculifer* & *G. ruber*	15.945	15.678-16.212

Table S2.

Principal Component Analysis (PCA) Results of major elements in core SCS-02

Elements	PC1	PC2
TiO_2	0.946	0.142
SiO_2	0.902	-0.341
K_2O	0.854	0.499
TFe_2O_3	0.752	0.586
Al_2O_3	0.742	0.542
MgO	-0.356	0.852
P_2O_5	-0.662	0.53
Na_2O	-0.675	0.453
CaO	-0.976	0.139
Variance (%)	61.411	25.037